



Layer-by-layer assembled magnetic prednisolone microcapsules (MPC) for controlled and targeted drug release at rheumatoid arthritic joints



Chakkarapani Prabu^a, Subbiah Latha^{a,*}, Palanisamy Selvamani^a, Fredrik Ahrentorp^b,
Christer Johansson^b, Ryoji Takeda^c, Yasushi Takemura^c, Satoshi Ota^d

^a Department of Pharmaceutical Technology & Centre for Excellence in Nanobio Translational Research, Anna University, Bharathidasan Institute of Technology Campus, Tiruchirappalli, Tamil Nadu, India

^b Acreo Swedish ICT AB, Arvid Hedvalls Backe 4, Göteborg, Sweden

^c Electrical & Computer Engineering & Faculty of Engineering Division of Intelligent Systems Engineering, Yokohama National University, Japan

^d Department of Electrical and Electronic Engineering, Shizuoka University, Japan

ARTICLE INFO

Keywords:

Prednisolone
Magnetic microcapsules
Layer-by-layer
Rheumatoid arthritis

ABSTRACT

We report here in about the formulation and evaluation of Magnetic Prednisolone Microcapsules (MPC) developed in order to improve the therapeutic efficacy relatively at a low dose than the conventional dosage formulations by means of magnetic drug targeting and thus enhancing bioavailability at the arthritic joints. Prednisolone was loaded to poly (sodium 4-styrenesulfonate) (PSS) doped calcium carbonate microspheres confirmed by the decrease in surface area from 97.48 m²/g to 12.05 of m²/g by BET analysis. Adsorption with oppositely charged polyelectrolytes incorporated with iron oxide nanoparticles was confirmed through zeta analysis. Removal of calcium carbonate core yielded MPC with particle size of ~3.48 μm, zeta potential of +29.7 mV was evaluated for its magnetic properties. Functional integrity of MPC was confirmed through FT-IR spectrum. Stability studies were performed at 25 °C ± 65% relative humidity for 60 days showed no considerable changes. Further the encapsulation efficiency of 63%, loading capacity of 18.2% and drug release of 88.3% for 36 h and its kinetics were also reported. The observed results justify the suitability of MPC for possible applications in the magnetic drug targeting for efficient therapy of rheumatoid arthritis.

1. Introduction

Novel drug delivery systems such as microspheres, nanoparticles, liposomes, micelles, emulsions have promising controlled drug release and cell or tissue specific targeting ability [1–4]. Recently, there has been increasing interest in developing multilayer coated microparticles with Layer-by-layer (LBL) methodology in order to achieve controlled drug release at the target site [5–8]. LBL method enables uniform and controlled multilayer film growth over diverse micro particles [9]. Calcium carbonate has widely been studied and used for biological applications due to its biocompatibility, biodegradability which prevents any unexpected adverse effects [10–12]. It has been reported that biomimetic mineralization method of preparation of CaCO₃ results in the formation of porous spherical microparticles with large surface area [13]. The porous texture of CaCO₃ affords to hold an increased pay load of small drug molecules and also aids controlled drug release [14,15]. Accordingly, CaCO₃ microparticles coated either with polysaccharides such as chitosan and alginate or polyelectrolytes such as poly (sodium 4-styrenesulfonate) (PSS), poly (allylamine hydrochloride) (PAH) have

already been investigated and reported for the possible applications in the controlled drug delivery [16–20]. Incorporating suitable magnetic materials to these microspheres were considered by many researchers, in order to assemble these drug carriers at a close proximity to the target site through application of an external magnetic field in order to improve the regional bioavailability [21]. Drug loaded hollow capsules have great potential due to their attributes such as superior drug encapsulation as well as release characteristics which can be fine-tuned as desired by varying and manipulating the capsule volume, capsule wall dimensions, the number of layers coated over the microspheres and also by varying the layer compositions [22].

Rheumatoid arthritis (RA) is an autoimmune disease characterized by chronic inflammation of synovial joints which leads to the destruction of articular tissue and the underlying bone on progression. As per an estimate, RA affects approximately 1% of the population worldwide [23–25]. RA therapy is customarily symptomatic and the medication includes steroids, nonsteroidal anti-inflammatory drugs, disease-modifying anti-rheumatic agents and immunosuppressant drugs [26]. Prednisolone is a synthetic glucocorticoid, a kind of cortisol which is

* Corresponding author.

E-mail address: lathasuba2010@gmail.com (S. Latha).

used to treat a variety of inflammatory conditions and rheumatoid arthritis [27]. Prednisolone is generally considered safe for human use at recommended doses, however, overdoses of prednisolone will result in sodium and water retention as well as adverse hypersensitivity including anaphylaxis, proximal myopathy, thromboembolism, hirsutism, dyspepsia and cardiovascular risks [28].

In the present study, the prepared porous PSS-doped calcium carbonate microspheres were used as templates for the encapsulation of prednisolone. Subsequently, alternatively coated with oppositely charged polyelectrolytes i.e., poly(allylamine hydrochloride) or Poly(sodium 4-styrenesulfonate) were coated over the microspheres. Heretofore, iron oxide magnetic nanoparticles as ferrofluid was incorporated in between the polyelectrolyte layers coated over the microspheres. Further, calcium carbonate template etching was realized by complexation with ethylenediaminetetraacetic acid (EDTA) solution yielding magnetic prednisolone microcapsule (MPC). The developed MPC can be employed for the controlled and targeted drug release in order to enhance the regional bioavailability and to minimize the adverse effects that arise due to use of high prednisolone doses.

2. Experimental section

2.1. Materials and methods

Prednisolone and all the chemicals and reagents used in this study were of analytical grade obtained from Sigma Aldrich India Pvt Ltd.

2.2. Preparation of magnetic prednisolone microcapsules

2.2.1. Preparation of PSS-doped CaCO₃ microspheres

Freshly prepared 0.2 M aqueous solution Na₂CO₃ (100 mL) was mixed with 400 mg of poly(sodium 4-styrenesulfonate). To the above, an aqueous solution of 0.2 M CaCl₂ (100 mL) was added and kept under constant stirring for 30 min at 4000 rpm. The obtained PSS-doped CaCO₃ microspheres were separated and dried in a vacuum oven at 50 °C for 1 h [29].

2.2.2. Drug loading into PSS-doped CaCO₃ microspheres

Prednisolone was loaded to PSS-doped CaCO₃ microspheres by solvent evaporation technique. Prednisolone (200 mg) was vortex dissolved in absolute ethanol (10 mL). Drug solution was transferred drop by drop to 400 mg of CaCO₃ microspheres dispersed in water and allowed to stand under constant stirring for 24 h. The drug loaded microspheres were recovered by centrifugation [15].

2.2.3. Preparation of ferrofluid

Ferrofluid was prepared using co-precipitation technique. Briefly, 2 M FeCl₃·6H₂O solution and 1 M FeCl₂·4H₂O solution were mixed under constant stirring in a magnetic stirrer at 750 rpm maintained at 80 °C in nitrogen atmosphere [30]. To the above, ammonia solution was added drop by drop till the formation of a black coloured precipitate which indicated the formation of magnetite nanoparticles as ferrofluid. The reaction mixture was kept under constant stirring for further 1 h and the pH of the solution was neutralized by repeated washing with deionised water.

2.2.4. Preparation of magnetic microcapsules

Magnetic prednisolone microcapsules were prepared in three steps, (Fig. 1).

In a first step, adsorption of oppositely charged polyelectrolytes (PAH/PSS) over the prednisolone loaded PSS-doped CaCO₃ microspheres using LBL technique. In a second step, incorporation of iron oxide magnetic nanoparticles in between the polyelectrolyte layers coated over PSS-doped CaCO₃ microspheres and finally removal of the CaCO₃ core from the PSS-doped CaCO₃ microspheres by etching with EDTA.

PAH (Mw~58,000)/PSS (Mw~70,000) polyelectrolyte solutions (2 mg/mL) were prepared with 0.5 M aqueous solution of sodium chloride and the pH was adjusted to 6.5 using sodium hydroxide solution. Previously dried prednisolone loaded PSS-doped CaCO₃ microspheres (0.2 g) were soaked in 0.5 M sodium chloride solution (10 mL) for 15 min. The drenched microspheres were then separated by centrifugation at 4000 rpm for 5 min. The microspheres separated as sediment were then mixed with 5 mL of PAH polyelectrolyte solution and incubated for 15 min with mild agitation in a vortex mixer. Unloaded polyelectrolytes were then removed by washing with sodium chloride (0.001 M) solution. After each loading cycle, the microspheres were washed thrice. After five cycles of polyelectrolyte coating layered alternatively, prednisolone loaded polyelectrolyte coated PSS-doped calcium carbonate microspheres were obtained. Previously, iron oxide magnetic nanoparticles were loaded in between the polyelectrolyte layers by adding and incubating the prepared ferrofluid for 15 min after the completion of the third cycle of polyelectrolyte coating. The remaining two cycles of polyelectrolyte loading was performed as detailed above. The PSS-doped CaCO₃ core was then removed selectively by adding 0.2 M EDTA solution of pH 6.5 and incubating the dispersion for 30 min and repeated twice yielded magnetic prednisolone microcapsules [31].

2.3. Evaluation studies

2.3.1. Physicochemical characterization

2.3.1.1. Surface morphology. The surface morphology of PSS-doped CaCO₃ microspheres and polyelectrolyte coated prednisolone loaded PSS-doped CaCO₃ magnetic microspheres were examined in a scanning electron microscope (JEOL-JSM 6701-F, Japan) after sputter coating using a thin layer of palladium-gold alloy [32].

The microstructural examination and morphology of the prepared iron oxide nanoparticles were observed in a Field Emission Transmission Electron Microscope (FE-TEM) (JEOL, JEM-2100F Transmission Electron Microscope, Japan) operated at 200 kV.

2.3.1.2. Particle size and zeta potential. Particle size and the zeta potential of iron oxide magnetic nanoparticles, PSS-doped CaCO₃ microspheres and MPC's were determined using Zetasizer Nano ZS, Malvern Instruments, Malvern, UK, Ver. 7.02. MPC was dispersed in deionized water (5 mL) and was loaded in a dip cell in order to minimize the impact of viscosity induced by the ingredients. The measurements were performed using 4 mW He-Ne laser (633 nm) as the light source at a fixed angle of 175°, and other operating conditions viz., medium refractive index 1.300, medium viscosity 0.8872 cP and temperature 25°C. ζ-Potential was calculated with a mix of laser doppler velocimetry and phase analysis light scattering (PALS). A Smoluchowsky constant F (Ka) of 1.5 had been used to determine potential values from the electrophoretic mobility. Results achieved were the average of three measurements [33].

2.3.1.3. Nanoparticle tracking analysis. Nanoparticle tracking analysis measurements were performed using NanoSight NS300 (Malvern Instruments, United Kingdom) system equipped with a high sensitivity CMOS camera and 532 nm laser. All measurements were performed at room temperature. The software used for capturing and analysing the data was the NTA 3.1 [34].

2.3.1.4. Surface area. The Brunauer, Emmett and Teller (BET) method was adapted for the determination of surface area and porosity of PSS-doped CaCO₃ microspheres and prednisolone loaded PSS-doped CaCO₃ microspheres with a BET analyzer (Nova-1000,

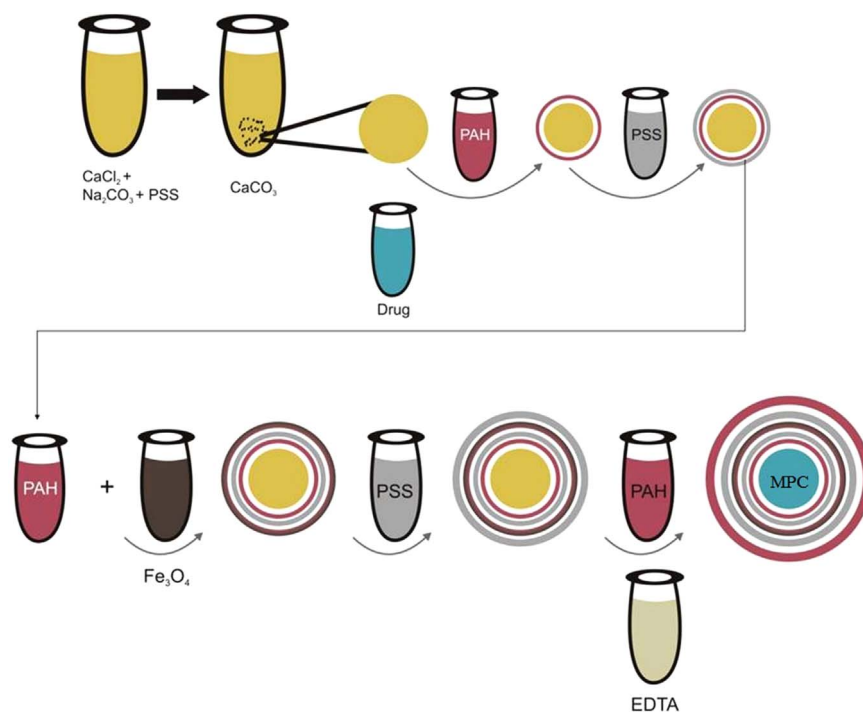


Fig. 1. Scheme for the preparation of magnetic prednisolone microcapsules.

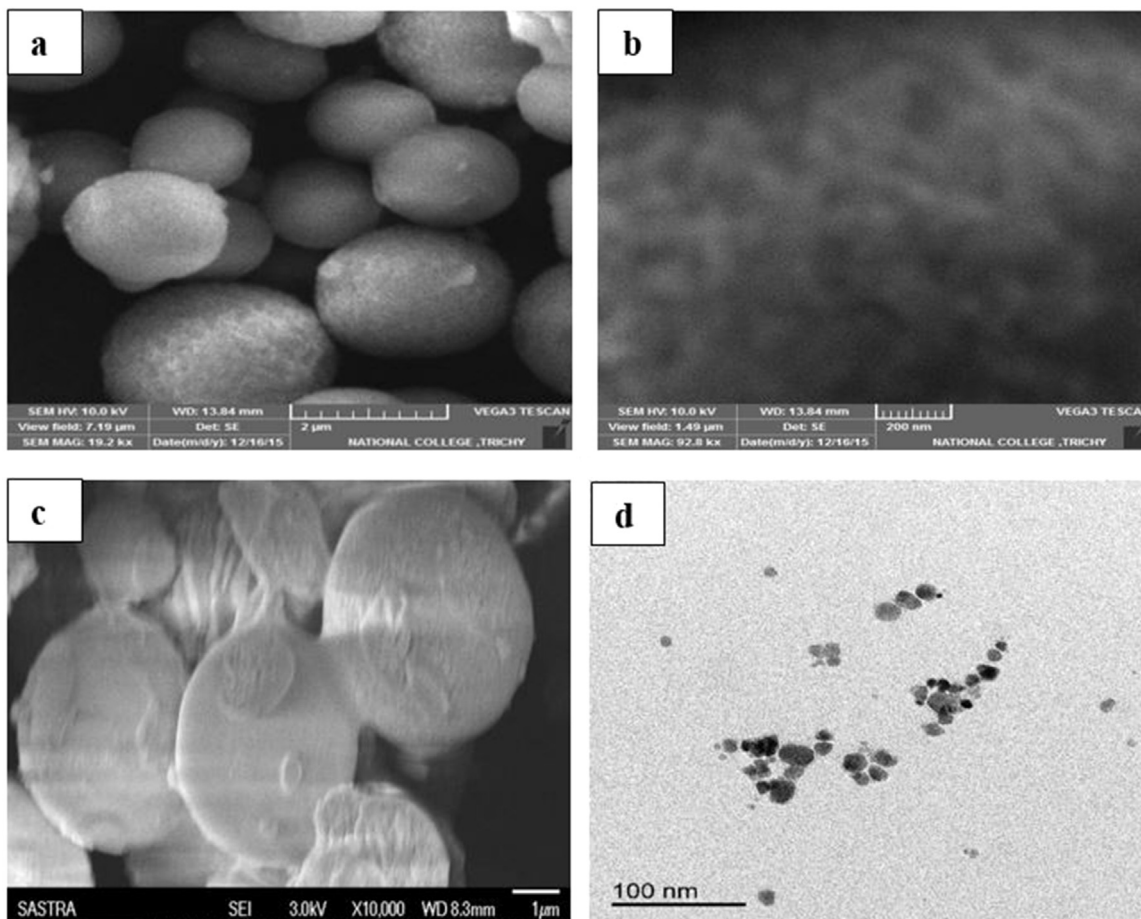


Fig. 2. (a) SEM image of PSS-doped CaCO_3 microspheres (b) Magnified SEM image of PSS-doped CaCO_3 microspheres with porous surface texture (c) SEM image of polyelectrolyte encapsulated PSS-doped CaCO_3 microspheres with smooth surface texture (d) TEM image of magnetic nanoparticles in the ferrofluid.

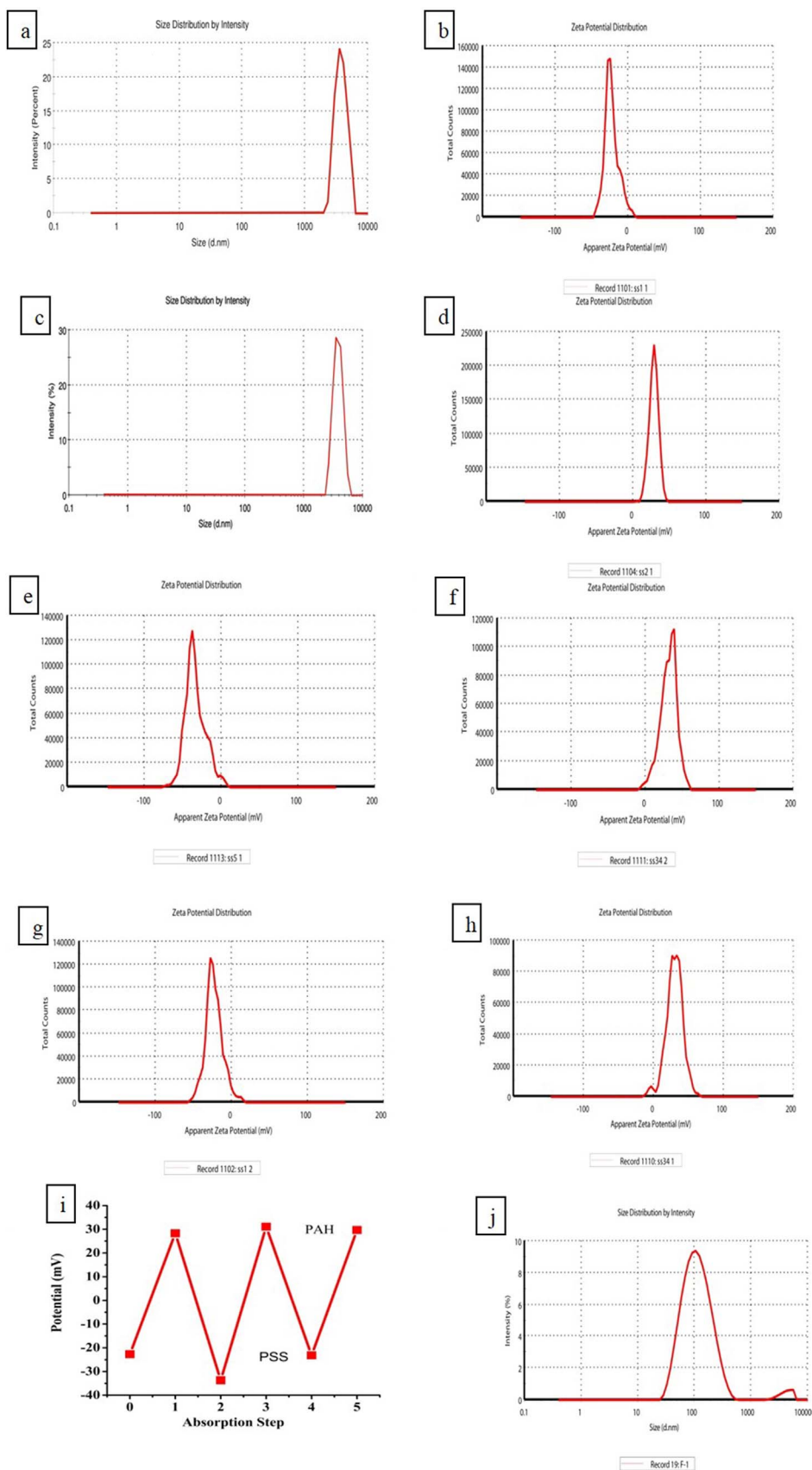


Fig. 3. (a-b) Particle size distribution and zeta potential of PSS doped CaCO_3 microspheres. (c) Size distribution of magnetic prednisolone microcapsules. (d-h) Zeta potential after addition of polyelectrolytes over PSS-doped CaCO_3 microspheres (Layers 1–5). (i) Graphical representation of switching of zeta potential over PSS-doped CaCO_3 microspheres. (j) Particle size distribution of Magnetic nanoparticles in ferrofluid.

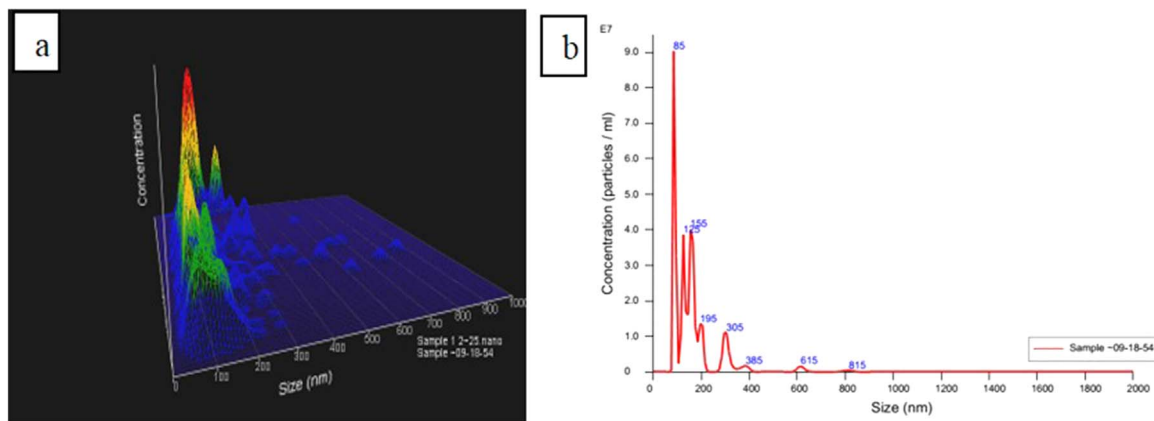


Fig. 4. (a) 3D image of size distribution of magnetic nanoparticles. (b) Size of magnetic nanoparticles.

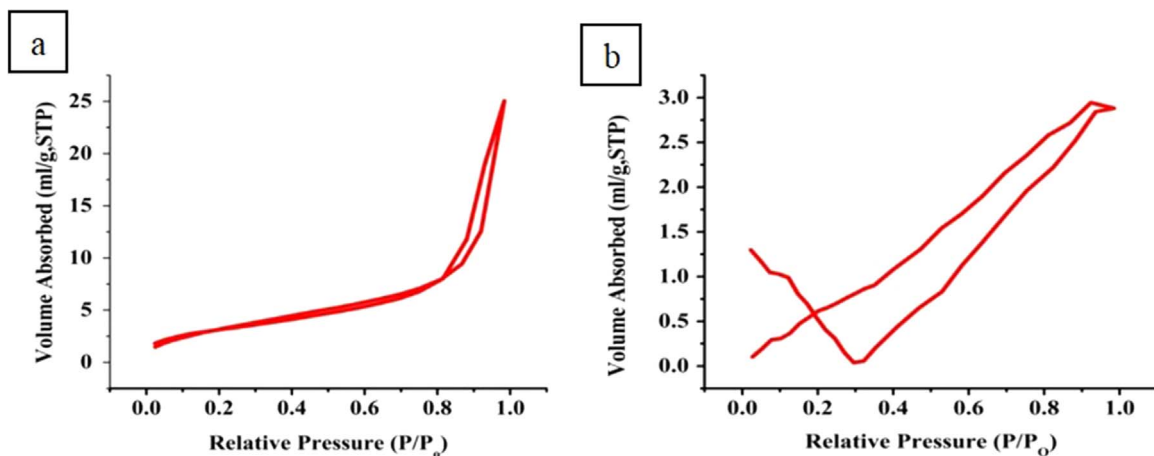


Fig. 5. N₂ absorption-desorption of PSS-doped CaCO₃ microspheres (a) before and (b) after prednisolone loading.

Table 1

BET characterization of porous PSS-doped CaCO₃ microspheres before and after drug loading.

PSS-doped CaCO ₃ microspheres	BET surface area (m ² /g)	Adsorption average (nm)	Total volume of pores at P/P ₀ (cc/g)
Before drug loading	97.48	3.19	0.0778
After drug loading	12.05	6.65	0.0200

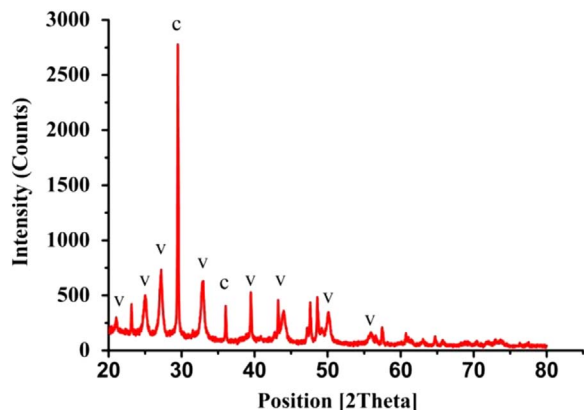


Fig. 6. XRD pattern of PSS-doped CaCO₃ microspheres.

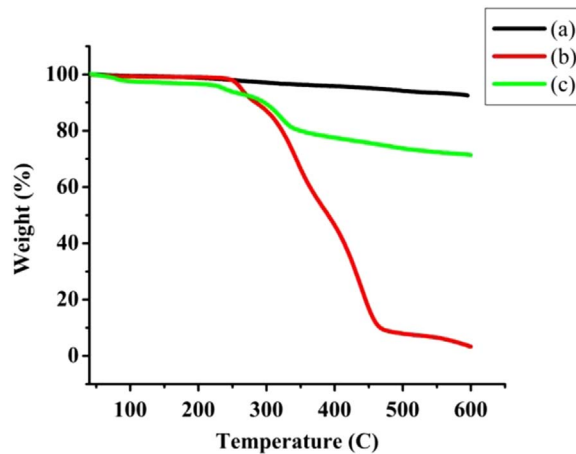


Fig. 7. Thermograms of (a) PSS-doped CaCO₃ microspheres (b) Prednisolone (c) Prednisolone loaded PSS-doped CaCO₃ microcapsules.

USA). The nitrogen sorption experiments were conducted prior to the analysis and the samples were outgassed at 200°C for at least 4 h [14].

2.3.1.5. *Crystallinity.* In order to confirm the crystalline state of the synthesised calcium carbonate, X-ray diffraction patterns of PSS-doped CaCO₃ microspheres were recorded on a powder X-Ray diffractometer (PW3040/60 X'pert PRO, PANalytical, Netherlands) in the 2θ range of 20–80° [14].

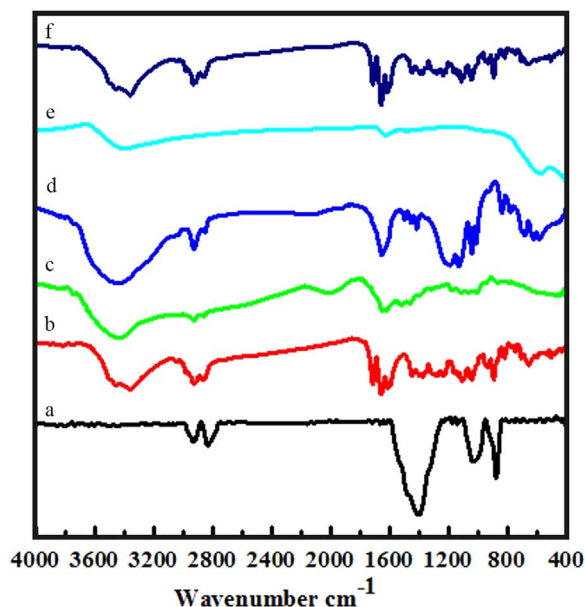


Fig. 8. FT-IR spectrums of (a) PSS-doped CaCO_3 microspheres (b) Prednisolone (c) PAH (d) PSS (e) Ferrofluid (f) Magnetic prednisolone microcapsules.

2.3.1.6. Thermal stability. The thermal stability of PSS-doped CaCO_3 microspheres, prednisolone loaded PSS-doped CaCO_3 magnetic microspheres and pure sample of prednisolone were examined using thermo-gravimetric analyzer (TGA) (TGA 4000 Perkin Elmer, USA). The thermograms were recorded at a temperature range from 35 to 800°C at a heating speed of 10°C/min under a constant flow of nitrogen atmosphere (20 mL/min) [15].

2.3.1.7. Chemical interactions. The FT-IR spectrum has been recorded on a FT-IR Spectrophotometer (Jasco 6300, Japan) for PSS-doped CaCO_3 microspheres, prednisolone, PAH, PSS, ferrofluid and MPC's in order to elucidate the possible chemical interactions between the drugs and excipients. The samples (5 mg) were mixed with potassium bromide (100 mg) in a mortar and compressed into pellets in a press was further loaded to the crystal sample holder and observed in the wavelength region of 4000–400 cm^{-1} at a resolution of 4 cm^{-1} [15].

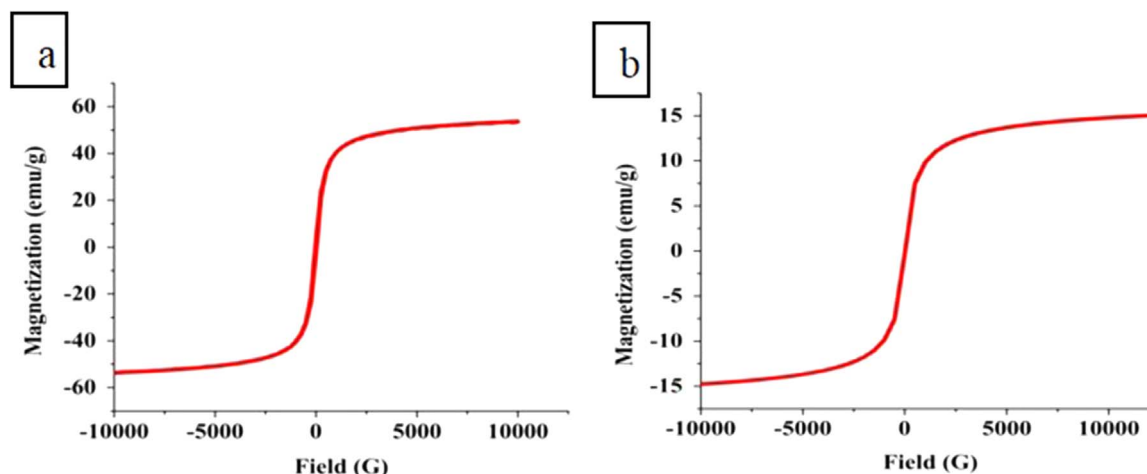


Fig. 9. Magnetization (in emu/g) as a function of magnetic field of (a) dried ferrofluid (b) dried MPC spheres at room temperature.

2.3.2. Magnetic characterization

2.3.2.1. Magnetometry. Magnetization vs Field property for iron oxide nanoparticles and MPC's were observed in a VSM system (Lakeshore Model 7404, USA) at 300 K [35].

2.3.2.2. AC susceptibility. The dynamic magnetic susceptibility measurements (i.e., AC magnetic susceptibility vs Frequency) for MPC's were done using the DynoMag system (Acreo Swedish ICT AB, Sweden) in a frequency range of 5–100 kHz. The AC susceptibility measurements are presented as the volume susceptibility (SI units) [33].

2.3.3. Pharmaceutical characterization

2.3.3.1. Encapsulation efficiency and loading capacity. Prednisolone (200 mg) was added to the PSS-doped CaCO_3 microspheres (200 mg) in 10 mL of the absolute ethanol and allowed to stand under stirring for 24 h for drug loading. This dispersion was then centrifuged at 2000 rpm results in the separation of the supernatant. The quantity of unloaded drug remained in the supernatant had been determined through UV–vis spectrophotometer (Shimadzu UV1800, Singapore) at 243 nm. The percent encapsulation efficiency was calculated as described below [36].

Encapsulation efficiency (%) = $[1 - (\text{Drug in supernatant (mg)} / \text{Total drug added (mg)})] \times 100$

MPC (200 mg) were digested with 20 mL of phosphate buffer pH 7.4 in a sonication bath (Model: 3.5 L 100 H, PCI analytics, India) and the solution was centrifuged at 2000 rpm for 30 min. The amount of prednisolone in MPC was determined as the difference between the total amount of drug used to prepare the MPC and the amount of drug present in the aqueous medium. The percent drug loading capacity was calculated as mentioned below [36].

Drug loading (%) = $[\text{Amount of drug in microcapsules (mg)} / \text{Amount of microcapsules recovered (mg)}] \times 100$.

2.3.3.2. Drug release pattern and release kinetics. The *in-vitro* drug release pattern of MPC's was studied in an open end tube sealed fitted with dialysis membrane (Himedia Laboratories Pvt. Ltd., India; core diameter 2.4 nm). The dialysis tube was attached to an USP dissolution apparatus (LABINDIA, India) filled with 1000 mL of buffer solution at pH 7.4 as dissolution medium, stirred at 60 rpm at 37°C. MPC's (200 mg) were placed inside the dialysis tube and aliquots of buffer

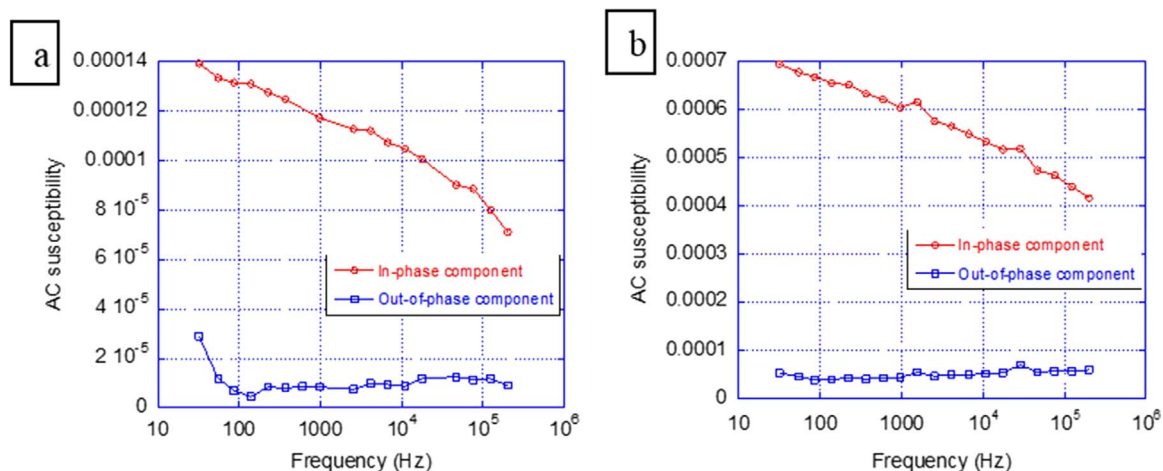


Fig. 10. (a) AC susceptibility versus frequency of magnetic susceptibility studies of MPC. (b) AC susceptibility versus frequency of magnetic nanoparticles in ferrofluid.

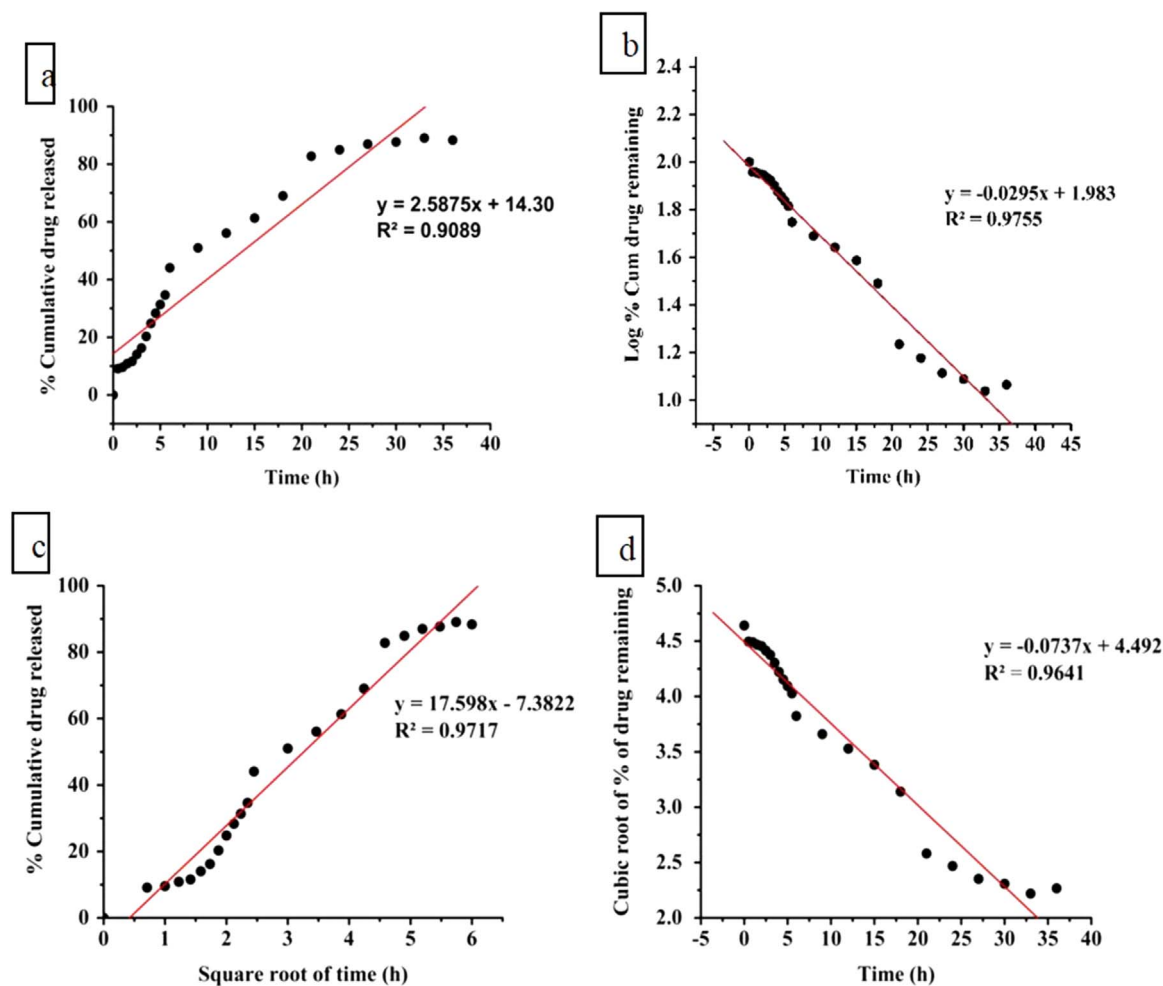


Fig. 11. Cumulative drug release pattern of MPC in different kinetic models (a) Zero order (b) First order (c) Higuchi (d) Hixson-Crowell.

(1 mL) were removed at fixed time durations from the dissolution medium outside the dialysis tube for a period of 36 h and an equivalent quantity of fresh buffer have been replaced. Absorbance of withdrawn aliquots was measured using double beam UV–vis spectroscopy at 243 nm. The amount of drug present in each aliquot was determined from the standard calibration graph. Data collected via *in-vitro* drug release studies had been integrated to the different kinetic equations, i.e., zero order, first order, Hixson Crowell and Higuchi equation. The release mechanism was evaluated with Peppas equation [37].

2.3.3.3. *Stability studies.* The formulated MPC had been presented to stability studies in amber and transparent airtight glass containers to estimate the stability of the formulation with respect to drug content and drug release characteristics after storing the multiple-units of the formulation in drug stability testing chamber (Model: WIL-195, Wadegati Lab Equip Pvt. Ltd., India) temperature was maintained at 25° C and 65% relative humidity for 60 days [37].

Table 2
Storage stability studies of magnetic prednisolone microcapsules.

S. No	Time (Days)	Size (μm)	Drug content (%)	Cumulative drug release (%)
1	0	3.48	97.19	89.27%
2	15	3.45	96.61	89.12%
3	30	3.44	96.24	89.03%
4	45	3.36	96.06	88.87%
5	60	3.31	95.69	88.48%

2.4. Results and discussion

2.4.1. Preparation of PSS-doped CaCO_3 microspheres

Porous PSS-doped CaCO_3 microspheres were prepared by biomimetalisation method. Development of the porous spherical non-agglomerating stable microspheres with uniform size has been a major task in this study. Mixing of Ca^{2+} and CO_3^{2-} forms an amorphous precipitate and on storage it turns into calcite aggregated particles with irregular shape [38–40]. Growth of the CaCO_3 spheres were controlled and influenced by strong binding interactions of polyanion PSS with Ca^{2+} ion. PSS precipitates together with the Ca^{2+} ions then the repulsive electrostatic force occur in between CaCO_3 and PSS ions which influences the development of pores in the PSS-doped CaCO_3 microspheres. Thus PSS plays the key role in the formation of the rough textured, porous, relatively monodisperse and spherical PSS-doped CaCO_3 microspheres without aggregation perhaps due to the co-crystallization of calcium with polyelectrolyte [14].

2.4.2. Preparation of magnetic prednisolone microcapsules

MPC's were successfully prepared after loading prednisolone and ferrofluid into the porous PSS-doped CaCO_3 microspheres, which were over coated alternatively using PAH or PSS by LBL technique. Subsequently, PSS-doped CaCO_3 core was successfully etch removed using EDTA yielding magnetic prednisolone microspheres.

2.5. Evaluation studies

2.5.1. Physicochemical characterization

2.5.1.1. Surface morphology. SEM images obtained for the PSS-doped CaCO_3 microspheres confirm that the particles obtained were spherical with porous surface texture (Fig. 2a and b). SEM image of the Prednisolone-loaded PSS-doped CaCO_3 microspheres encapsulated with five bilayers of PAH/PSS is presented in (Fig. 2c). The surface texture of the polyelectrolyte over coated microspheres seems significantly smooth pattern with slight agglomeration among them. This could be due to the linking of oppositely charged PAH and PSS chains adsorbed on the surrounding particles [41–47]. The transformation of porous texture to smooth texture confirms the surface coating with alternate polyelectrolytes.

The TEM images of the prepared iron oxide (magnetite) nanoparticles showed a ferrofluid consisting of nanoparticles in the size range of ~ 10 nm (Fig. 2d).

2.5.1.2. Particle size and Zeta potential. The mean hydrodynamic diameter of the PSS-doped CaCO_3 microspheres were ~ 4.06 μm (Fig. 3a) with a poly dispersity index of 0.233 and exhibited a zeta potential of -22.7 mV (Fig. 3b) which implies the prepared microspheres were relatively monodisperse and stable.

The particle size of the developed MPC's were ~ 3.48 μm with a polydispersity index of 0.233 (Fig. 3c) implies that the prepared

microcapsules were relatively monodisperse and stable. The revealed polydispersity index is an effective sign of long-term colloidal stability of the encapsulated MPC. The noticeable shifting of ζ -potential confirms alternative deposition of the polycation PAH and polyanion PSS in the prednisolone-loaded PSS-doped CaCO_3 microspheres and in addition microspheres had been encapsulated (Fig. 3d-h). The prepared MPC's exhibited a positive zeta potential of $+29.7$ (Fig. 3h). The pattern of zeta potential change after inclusion of polyelectrolyte layer for five cycles with alternative charge over PSS-doped CaCO_3 microspheres was indicated (Fig. 3i). The observed reduction in the mean size of MPC's probably occurs as a result of hydrolyzation of the CaCO_3 [14]. Mean particle diameter of the prepared iron oxide magnetic nanoparticles were ~ 91.8 nm (Fig. 3j).

2.5.1.3. Nanoparticle tracking analysis (NTA). The results obtained with NTA were shown in (Fig. 4a and b) the size and size distribution of iron oxide magnetic nanoparticles [34].

2.5.1.4. Surface area. The adsorption–desorption isotherms obtained for the PSS-doped CaCO_3 microspheres and prednisolone loaded PSS-doped CaCO_3 microspheres through BET analysis confirmed the prednisolone loading into the nanopores of the PSS-doped CaCO_3 microspheres (Fig. 5a and b).

Further, specific surface area, pore size and pore volume distribution values for the microspheres before and after drug loading are given in Table 1. The BET surface area (S_{BET}) of PSS-doped CaCO_3 microspheres was 97.48 m^2/g . As a result of prednisolone loading, the BET surface area of the PSS-doped CaCO_3 microspheres was reduced to 12.05 m^2/g and the pore volume was dropped from 0.0778 to 0.0200 cc/g , proposing the penetration of the prednisolone molecules inside the nanopores [48–50].

It could be that, prednisolone along with PSS-doped CaCO_3 microspheres are hugely enlarged and effectively charged. Hence, the gaps in between the CaCO_3 nanocrystals are preferentially filled by prednisolone and turned smaller, clarifies the reason for the increase in adsorption average diameter from 3.19 to 6.65 nm after loading [15].

2.5.1.5. Crystallinity. The XRD pattern shows (Fig. 6) that the PSS-doped CaCO_3 microspheres had a phase that is dominant of vaterite, although a trace quantity of calcite also existed. The diffraction that is with broadening peaks suggests that the produced vaterite microspheres consisted of miniature nanoparticles. Recrystallization of the PSS-doped CaCO_3 microspheres that is porous composed of carbonate nanoparticles was blocked by the PSS adsorbed on the surface of the carbonate nanoparticles. Thus, PSS-doped CaCO_3 microspheres were much more stable than those without additives [49,50].

2.5.1.6. Thermal stability. Thermograms of the PSS-doped CaCO_3 microspheres, prednisolone and prednisolone loaded PSS-doped CaCO_3 microspheres were presented (Fig. 7). The percent weight loss for PSS-doped CaCO_3 microspheres, prednisolone and prednisolone loaded PSS-doped CaCO_3 microspheres were 7.47% , 96.71% and 28.96% respectively when observed at 600°C . The reason seems to be that most adsorbed prednisolone stays in the pores and not at the external surface enhancing the resistance to the thermo-decomposition and that the decomposed prednisolone residues remain in the pore inner of the porous CaCO_3 microspheres and cannot undergo a complete phase transition to vapour state [15].

2.5.1.7. Chemical interactions. FT-IR spectroscopy explains that no

chemical interactions exist in between the prednisolone and employed excipients. FT-IR spectrum of PSS-doped CaCO₃ microspheres (Fig. 8a) shows characteristic CaCO₃ bands located at 1401 cm⁻¹, 872 cm⁻¹ and 749 cm⁻¹ which were characterized to be the usual bands of the carbonate ions in calcium carbonate, along with the related bands at 2925 cm⁻¹, 2830 cm⁻¹ probably results from the asymmetric and symmetric CH stretching indicates the occurrence of PSS [51]. The characteristic peaks of prednisolone (Fig. 8b) showed the principal peaks at 1608 cm⁻¹ (carbonyl group), 3356 cm⁻¹ (OH stretching), 2862 cm⁻¹ (CH stretching) and 1039 cm⁻¹ (OH bending) confirming the purity of the drug as per established standards [52]. FT-IR spectral analysis of PAH (Fig. 8c) was observed at 3441 cm⁻¹ (aliphatic amine NH stretching), 1519 cm⁻¹ (aliphatic amine NH bending) and 2924 cm⁻¹ (CH₂ stretching). FT-IR spectra of PSS (Fig. 8d) showed peaks at 1186 cm⁻¹, 1039 cm⁻¹ could be assigned to the SO₃ group (antisymmetric and symmetric vibrational absorption) and 1128 cm⁻¹ from the inplane skeleton vibration of the benzene ring respectively [53]. An infrared spectrum of the ferrofluid (Fig. 8e) was characterized with the bands at 567 cm⁻¹, due to the Fe-O bond in tetrahedral and octahedral positions [54]. The spectral group frequencies of MPC's (Fig. 8f) were characterized at 3453 cm⁻¹ (aliphatic amine NH stretching), 1610 cm⁻¹ (aliphatic amine NH bending) and 2981 cm⁻¹ (CH₂ stretching). Peaks for the PSS-doped CaCO₃ core material, does not exist it conforms the removal of core.

2.5.2. Magnetic characterization

2.5.2.1. Magnetometry. DC magnetization studies were carried out using vibrating sample magnetometer (VSM) to examine the static magnetic characteristics of the magnetic particles (both the ferrofluid and the MPC) at room temperature. (Fig. 9a and b), reveals the hysteresis curves of dried ferrofluid and dried MPC's. From the results the saturation magnetization of the ferrofluid were 51.11 emu/g (Fig. 9a) and saturation magnetization of the MPC's were 15.02 emu/g (Fig. 9b). This unique superparamagnetic activity of MPC's is suitable for the magnetic drug targeting applications [55,56].

2.5.2.2. AC susceptibility. The result of AC susceptibility versus frequency analysis of samples MPC's and magnetic nanoparticles are presented in the section. All measurements were carried out at 25 °C. The in-phase (real part) and out-of-phase (imaginary part) components of samples MPCs and magnetic nanoparticles are shown in (Fig. 10a and b). Both of these samples show a tendency of particle agglomeration and a major part of the particles were seen to sediment to the bottom of the sample tube after the measurement. The particles that sediment cannot rotate and thus can only show internal Néel relaxation within each magnetic core (nanocrystal). Due to the exponential dependence between the core volume and the Néel relaxation time, even a narrow core size distribution can give a large distribution in relaxation times. A large distribution in relaxation times will give a large width in relaxation frequencies in the AC susceptibility spectra. This can be seen both for sample MPCs and magnetic nanoparticles with almost non-zero and constant values of the out-of-phase component and a decline in the in-phase component in the whole measured frequency range. However, there is a build-up of a relaxation at low frequencies (starting in the range of 30 Hz) for MPCs (Fig. 10a) and this can be attributed to that some of the particles are still in dispersion and can rotate and show Brownian relaxation. The full Brownian relaxation peak in the out-of-phase component will be below 30 Hz. A Brownian relaxation frequency of 30 Hz corresponds to a particle size of 240 nm, but since the full relaxation peak is below 30 Hz the particle size is larger. If we assume that Brownian relaxation peak is in the range of 1 Hz this corresponds to a particle size of

750 nm [33].

2.5.3. Pharmaceutical characterization

2.5.3.1. Encapsulation efficiency and loading capacity. Prednisolone permeate and gets entrapped into core of PSS-doped CaCO₃ microparticles along with solvent facilitated a comprehensive pore filling with an encapsulation efficiency of 63% and drug loading capacity of 18.2%.

2.5.3.2. Drug release pattern and release kinetics. *In-vitro* drug release profile of MPC was observed using dialysis bag by adapting dialysis method. Maximum release of 88.3% of prednisolone was observed in 200 mg of the microcapsules after 36 h. Drug release kinetics were obtained by substituting the *in-vitro* release data in equations of zero order, first order, Higuchi and Hixson-Crowell models (Fig. 11a–d). The correlation coefficient values for zero order, first order, Higuchi and Hixson-Crowell models were 0.90, 0.97, 0.97 & 0.96 respectively. Both first order and Higuchi model shows the finest fit to drug release kinetics based upon the correlation coefficient. Their linearity had been found in the square root of time versus cumulative percentage of drug released (Fig. 11c) showed that the drug release may possibly be happened from the inner core of the microcapsules through diffusion, on the another hand the graphical representation of the time versus cube Log % cum drug remaining shows the relationship explains the release from the porous matrices (Fig. 11d) [57,58]. Therefore, to understand upon the drug release rate from the microcapsules is not just restricted by the drug particles dissolution rate but further by the diffusion.

2.5.3.3. Stability studies. Storage stability studies on different physicochemical and pharmaceutical parameters were performed at 25 °C ± 65% relative humidity for 60 days are given in Table 2. No considerable changes were observed throughout the duration of studies [33].

3. Conclusion

Thus in the current study utilizing the adsorption capacity of PSS doped CaCO₃ microspheres and its further development as multi-layered polyelectrolyte microcapsules encapsulated with prednisolone and magnetite was described. Moreover, it has been proven that the multilayer coating has the ability to prolong the release of the loaded prednisolone within the incubation time. Hence, we would like to conclude that this system holds great application potential for the use in *in-vivo* drug delivery for rheumatoid arthritis magnetic targeted therapy.

Acknowledgements

The work was supported by the research grants sanctioned to Dr.S.Latha and Dr.P.Selvamani from the Defence Research and Development Organization, New Delhi (No. ERIP/ER/0903779/M/01/1249), Government of India. FT-IR and Particle size cum Zeta potential measurements of this work were utilized from National Facility for Drug Development for Academia, Pharmaceutical and Allied Industries, Anna University, BIT Campus, Tiruchirappalli sponsored by the Department of Science and Technology, New Delhi. The authors acknowledges the support extended by Dr.Namrata Jain.

Mr. Prince Sahay, Mr.P.S.Radahakrishnan of M/s. Aimil-Malvern India Pvt Ltd, New Delhi, for NTA using Nanosight 300.

References

- [1] S. Benita, *Microencapsulation Drugs and the Pharmaceutical Science*, Marcel Dekker, New York, 1996.
- [2] T.M. Allen, P.R. Cullis, Drug delivery systems: entering the mainstream, *Science* 303 (2004) 1818–1822.
- [3] I. Brigger, C. Dubernet, P. Couvreur, Nanoparticles in cancer therapy and diagnosis, *Adv. Drug Deliv. Rev.* 54 (2002) 631–651.
- [4] V.P. Torchilin, Recent advances with liposomes as pharmaceutical carriers, *Nat. Rev. Drug Discov.* 4 (2005) 145–160.
- [5] A.A. Antipov, G.B. Sukhorukov, E. Donath, H. Mohwald, Sustained release properties of polyelectrolyte multilayer capsules, *J. Phys. Chem. B* 105 (2001) 2281–2284.
- [6] X. Qiu, S. Leporatti, E. Donath, H. Mohwald, Studies on the drug release properties of polysaccharide multilayers encapsulated ibuprofen microparticles, *Langmuir* (17) (2001) 5375–5380.
- [7] S. Ye, C. Wang, X. Liu, Z. Tong, B. Ren, F. Zeng, New loading process and release properties of insulin from polysaccharide microcapsules fabricated through layer-by-layer assembly, *J. Control. Release* 112 (2006) 79–87.
- [8] C. Wang, S. Ye, L. Dai, X. Liu, Z. Tong, Enhanced resistance of polyelectrolyte multilayer microcapsules to pepsin erosion and release properties of encapsulated indomethacin, *Biomacromolecules* 8 (2007) 1739–1744.
- [9] G.B. Sukhorukov, E. Donath, H. Lichtenfeld, E. Knippel, M. Knippel, A. Budde, H. Mohwald, Layer-by-layer self assembly of polyelectrolytes on colloidal particles, *Colloid Surf. A* 137 (1998) 253–266.
- [10] L. Wang, Z. Meng, Y. Yu, Q. Meng, D. Chen, Synthesis of hybrid linear-dendritic block copolymers with carboxylic functional groups for the biomimetic mineralization of calcium carbonate, *Polymer* 49 (2008) 1199–1210.
- [11] G. Wang, L. Li, J. Lan, L. Chen, J. You, Biomimetic crystallization of calcium carbonate spherulites controlled by hyperbranched polyglycerols, *Mater. Chem.* 18 (2008) 2789–2797.
- [12] Y. Yao, W. Dong, S. Zhu, X. Yu, D. Yan, Novel morphology of calcium carbonate controlled by poly (L-lysine), *Langmuir* (2009) 13238–13243.
- [13] W. Wei, G.H. Ma, G. Hu, D. Yu, T. McLeish, Z.G. Su, Z.Y. Shen, Preparation of hierarchical hollow CaCO₃ particles and the application as anticancer drug carrier, *J. Am. Chem. Soc.* (2008) 15808–15810.
- [14] C. Peng, Q. Zhao, C. Gao, Sustained delivery of doxorubicin by porous CaCO₃ and chitosan/alginate multilayers-coated CaCO₃ microparticles, *Colloids Surf. A-Physicochem. Eng. Asp.* 353 (2010) 132–139.
- [15] C.Y. Wang, C.Y. He, Z. Tong, X.X. Liu, B.Y. Ren, F. Zeng, Combination of adsorption by porous CaCO₃ microparticles and encapsulation by polyelectrolyte multilayer films for sustained drug delivery, *Int. J. Pharm.* 308 (2006) 160–167.
- [16] Y. Zhao, Y. Lu, Y. Hu, J.P. Li, L. Dong, L.N. Lin, S.H. Yu, Synthesis of superparamagnetic CaCO₃ mesocrystals for multistage delivery in cancer therapy, *Small* 6 (2010) 2436–2442.
- [17] J. Wang, J.S. Chen, J.Y. Zong, D. Zhao, F. Li, R.X. Zhuo, S.X. Cheng, Calcium carbonate/carboxymethyl chitosan hybrid microspheres and nanospheres for drug delivery, *J. Phys. Chem. C* 114 (2010) 18940–18945.
- [18] X. Shi, F. Caruso, Release Behavior of Thin-Walled Microcapsules Composed of Polyelectrolyte Multilayers, *Langmuir* 17 (2001) 2036–2042.
- [19] O.P. Tiourina, G.B. Sukhorukov, Multilayer alginate/protamine microcapsules: encapsulation of alpha-chymotrypsin and controlled release study, *Int. J. Pharm.* 242 (2002) 155–161.
- [20] H. Trotter, A.A. Zaman, R. Partch, Preparation and characterization of polymer composite multilayers on SiO₂, *J. Colloid Interface Sci.* 286 (2005) 233–238.
- [21] S. Sadasivan, G.B. Sukhorukov, Fabrication of hollow multifunctional spheres containing MCM-41 nanoparticles and magnetite nanoparticles using layer-by-layer method, *J. Colloid Interface Sci.* 304 (2006) 437.
- [22] C.S. Peyratout, L. Dahne, Tailor-made polyelectrolyte microcapsules: from multi-layers to smart containers, *Angew. Chem. Int. Ed.* 43 (2004) 3762–3783.
- [23] L. Bao, Y. Zhu, A.M. ElHassan, Q. Wu, B. Xiao, J. Zhu, U. Lindgren, Adjuvant-induced arthritis: il-1 α , IL-6 and TNF- α are up-regulated in the spinal cord, *Neuroimmunology, Neuroreport* 12 (18) (2001) 3905–3908.
- [24] S.D. Gauldie, D.S. McQueen, C.J. Clarke, I.P. Chessell, A robust model of adjuvant-induced chronic unilateral arthritis in two mouse strains, *J. Neurosci. Methods* 139 (2004) 281–291.
- [25] F. Rannou, M. Francois, M.T. Corvol, F. Berenbaum, Cartilage breakdown in rheumatoid arthritis, *Jt. Bone Spine* 73 (2006) 29–36.
- [26] R. Mythilypriya, P. Shanthi, P. Sachdanandam, Salubrious effect of kalpaamruthaa, a modified indigenous preparation in adjuvant induced arthritis in rats—a biochemical approach, *Chem. Biol. Interact.* 173 (2) (2008) 148–158.
- [27] M. Davis, Prednisone or Prednisolone for the treatment of chronic active hepatitis A comparison of plasma availability, *Br. J. Clin. Pharmacol.* 5 (1978) 501–505.
- [28] K. Meeran, Glucocorticoid replacement, *Br. Med. J.* 349 (2014) 4843.
- [29] Z. Lu, J. Zhang, Y. Ma, S. Song, W. Gu, Biomimetic mineralization of calcium carbonate/carboxy methylcellulose microspheres for lysozyme immobilization, *Mater. Sci. Eng. C* 32 (2012) 1982–1987.
- [30] S. Ghassabian, T. Ehtezazi, S.M. Forutan, S.A. Mortazavi, Dexamethasone loaded magnetic albumin microspheres preparation and in-vitro release, *Int. J. Pharm.* 130 (1996) 49–66.
- [31] S.H. Hu, C.H. Tsai, C.F. Liao, D.M. Liu, S.Y. Chen, Controlled rupture of magnetic polyelectrolyte microcapsules for drug delivery, *Langmuir* 24 (2008) 1181–1188.
- [32] Y. Jin, W. Liu, J. Wang, J. Fang, H. Gao, (Protamine/dextran sulfate)₆ microcapsules templated on biocompatible calcium carbonate microspheres, *Colloid Surf. A* 342 (2009) 40–45.
- [33] C. Prabu, S. Latha, P. Selvamani, B. Arputha, A. Fredrik, J. Christian, J. Christer, Encapsulation of methotrexate loaded magnetic microcapsules for magnetic drug targeting and controlled drug release, *J. Magn. Magn. Mater.* 380 (2015) 285–294.
- [34] M. Tong, O.S. Brown, P.R. Stone, L.M. Cree, L.W. Chamley, Flow speed alters the apparent size and concentration of particles measured using NanoSight nanoparticle tracking analysis, *Placenta* 38 (2016) 29–32.
- [35] J. Yang, S.B. Park, H.G. Yoon, Y.M. Huh, S. Haam, Preparation of poly - caprolactone nanoparticles containing magnetite for magnetic drug carrier, *Int. J. Pharm.* 324 (2006) 185–190.
- [36] L.N. Ramana, S. Sethuraman, U. Ranga, U.M. Krishnan, Development of a liposomal nanodelivery system for nevirapine, *J. Biomed. Sci.* 17 (2010) 1–9.
- [37] S. Latha, P. Selvamani, C. SenthilKumar, P. Sharavanan, G. Suganya, V.S. Beniwal, P.R. Rao, Formulation development and evaluation of metronidazole magnetic nanosuspension as a magnetic-targeted and polymeric-controlled drug delivery system, *J. Magn. Magn. Mater.* 321 (2009) 1580–1585.
- [38] T. Kato, T. Susuki, T. Amamiya, T. Irie, M. Komiyama, H. Yui, Effects of Macromolecules on the crystallization of CaCO₃ the formation of organic/inorganic composites, *Supramol. Sci.* 5 (1998) 411–415.
- [39] F. Manoli, E.J. Dalas, Spontaneous precipitation of calcium carbonate in the presence of ethanol, isopropanol and diethylene glycol, *Cryst. Growth* 218 (2000) 359–362.
- [40] H. Colfen, L. Qi, A systematic examination of the morphogenesis of calcium carbonate in the presence of a double-hydrophilic block copolymer, *Chem.-A Eur. J.* 7 (1) (2001) 106–116.
- [41] L.S. Tracy, C.J.P. Francúois, H.M.J. Jennings, The growth of calcite spherulites from solution: I. Experimental design techniques, *J. Cryst. Growth* (1998) 374–381.
- [42] N. Koga, Y. Nakagoe, H. Tanaka, Crystallization of amorphous calcium carbonate, *Thermochim. Acta* (1998) 239–244.
- [43] D. Horn, Rieger, organic nanoparticles in the aqueous phase-theory, experiment, and use, *Angew. Chem. Int. Ed.* (2001) 4330–4361.
- [44] T. Ogino, T. Suzuki, K. Sawad, The formation and transformation mechanism of calcium carbonate in water, *Geochim. Cosmochim. Acta* 51 (1987) 2757–2767.
- [45] N. Spanos, P.G.J. Koutsoukos, The transformation of vaterite to calcite: effect of the conditions of the solutions in contact with the mineral phase, *J. Cryst. Growth* (1998) 783–790.
- [46] M.J. Kitamura, Crystallization and transformation mechanism of calcium carbonate polymorphs and the effect of magnesium ion, *Colloid Interface Sci.* 236 (2001) 318–327.
- [47] M. Kitamura, H. Konno, A. Yasui, H. Masuoka, Controlling factors and mechanism of reactive crystallization of calcium carbonate polymorphs from calcium hydroxide suspensions, *J. Cryst. Growth* (2002) 323–332.
- [48] J.H. De Boer, *Dynamical Character of Adsorption*, Clarendon Press, United Kingdom, 1953.
- [49] D.V. Volodkin, N.I. Larionova, G.B. Sukhorukov, Protein encapsulation via porous CaCO₃ microparticles templating, *Biomacromolecules* (5) (2004) 1962–1972.
- [50] D.V. Volodkin, A.I. Petrov, M. Pevrt, G.B. Sukhorukov, Matrix polyelectrolyte microcapsules: new system for macromolecule encapsulation, *Langmuir* 20 (2004) 3398–3406.
- [51] Y. Wang, Y.X. Moo, C. Chen, P. Gunawan, R. Xu, Fast precipitation of uniform CaCO₃ nanospheres and their transformation to hollow hydroxyapatite nanospheres, *J. Colloid Interf. Sci.* 352 (2010) 393–400.
- [52] D. Arun, N. Venugopal, L. Shekar, B. Ramarav, J.V. Rao, K. Karunakar, Y. Surendra, Formulation, characterization and in vitro evaluation of orodispersible taste masking tablets of prednisolone sodium phosphate, *IJPBS* 2 (2012) 30–41.
- [53] J.C. Yang, M.J. Jablonsky, J.W. Mays, NMR and FT-IR studies of sulfonated styrene-based homopolymers and copolymers, *Polymer* 43 (2002) 5125–5132.
- [54] P.E.G. Casillas, C.A.R. Gonzalez, C.A.M. Perez, *Infrared Spectroscopy of Functionalized Magnetic Nanoparticles. Infrared spectroscopy - Materials Science, Engineering and Technology Prof. Theophanides Theophile (Ed.)*. (2012) 405–420
- [55] T.H. Hai, L.H. Phuc, D.T.K. Dung, N.T.L. Huyen, B.D. Long, L.K. Vinh, N.T.T. Kieu, Contrast agents for magnetic resonance imaging based on ferrite nanoparticles synthesized by using a wet-chemical method, *J. Korean Phys. Soc.* 53 (2008) 772–775.
- [56] M.H.R. Farimani, N. Shahtahmassebi, M.R. Roknabadi, N. Ghows, Synthesis and study of structural and magnetic properties of super paramagnetic Fe₃O₄@SiO₂ core/shell nanocomposite for biomedical applications, *Nanomed. J.* 1 (2014) 71–78.
- [57] P. Costa, J.M.S. Lobo, Modeling and comparison of dissolution profiles, *Eur. J. Pharm. Sci.* 13 (2001) 123–133.
- [58] P.J. Flory, J. Rehner Jr., Statistical mechanics of cross-linked polymer networks II. Swelling, *J. Chem. Phys.* 11 (1943) 521–526.